Zeeman effect

Robin Kugic, Alexander Moor
Praktikum für Fortgeschrittene
Universität des Saarlandes

August 20, 2024

Inhaltsverzeichnis

0 Introduction

In the following experiment, we took a closer look at the Zeeman effect. To start with, let's understand what the Zeeman effect actually is. The Zeeman effect was first discovered by its namesake, Pieter Zeeman, in 1896. He observed that when you place an incandescent lamp, for example, in a homogeneous magnetic field and look at the spectral lines, you notice that as you increase the magnetic field, the spectral lines initially broaden and then, with further increase, eventually split into multiple energy levels. Today, we also have an explanation for this. In the following sections, we will delve deeper into the description of the effect, look at what exactly we aim to investigate, and describe our experimental setup. We will observe the spectral lines splitting up into the D_1- and D_2-lines and determine the Landé-factors and Clebsch-Gordan-coefficients.

1 Zeeman effect

1.1 Explanation

We now have a general understanding of what the Zeeman effect is and what is observed, but we also need to know why this happens. For that, let's look at the structure of an atom. We have the atomic nucleus with neutrons and protons, and surrounding it are the electrons. These are the crucial particles we need to examine. The electrons are described by quantum numbers:

- Principal quantum number n
- Azimuthal (angular momentum) quantum number
- Magnetic quantum number m
- Spin quantum number s.

These play an important role in the Zeeman effect because they provide us with selection rules and possible transitions, etc. We irradiate our atoms with light (energy), causing an electron in the atom to be elevated from an energy level n to an energy level (n+1), meaning it absorbs energy. This atom also releases the energy and returns from the excited state to the normal state, emitting energy in the form of a photon. The frequencies are identical unless an external magnetic field is applied. In that case, the frequencies change, and we observe the splitting of the spectral lines. This happens because the electrons in the energy levels have different magnetic quantum numbers m, resulting in differently oriented magnetic dipoles. When the magnetic field is applied, they align, and energy is lost since the energy depends on the orientation of the particle in the magnetic field. Thus, we have multiple particles on the same energy level but with different orientations and energies, which changes the frequencies and explains the splitting of the spectral lines.

This can be indicated in Figure 1. Now we can further distinguish between:

- normal Zeeman-Effect

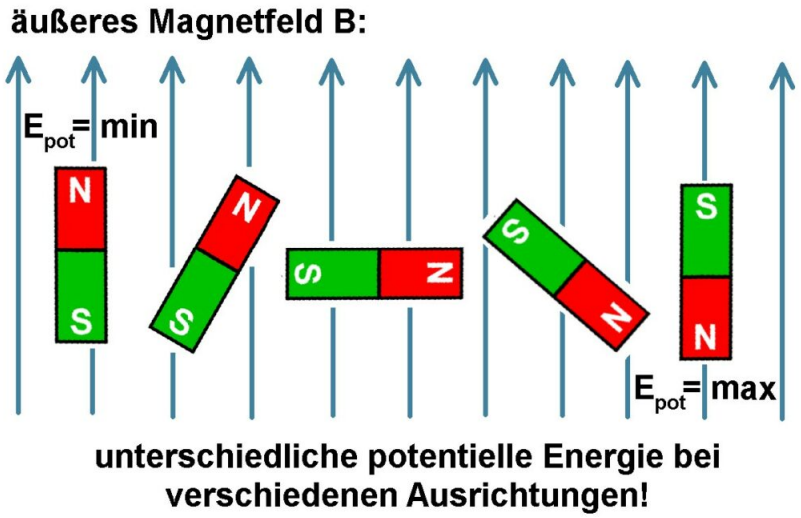

Figure 1: Ausrichtung der magnetischen Dipole im Magnetfeld

- anomalous Zeeman-Effect
- Paschen-Becken-Effect

1.2 Normal Zeeman-Effect

The normal Zeeman effect occurs in atomic transitions where the total spin is 0, meaning there is an even number of electrons. Thus, this depends on the spin quantum numbers. In this case, the splitting of the spectral line occurs symmetrically into only three components(es gilt $\Delta m_J = 0, \pm 1$) Why this is the case will be explained later when we discuss the selection rules.

1.3 Anomalous Zeeman-Effect

In the anomalous Zeeman effect, the atomic transition occurs when the total spin $\neq 0$. This results in the spectral lines splitting not just into three, but into multiple spectral lines, depending on the possible Δm_J values.

1.4 Paschen-Becken-Effekt

This occurs in very strong magnetic fields when the Zeeman splitting is greater than the fine structure splitting. In this case, the influence of the spin state is reduced, and the splitting follows the l and s quantum numbers.
Since we are using a sodium lamp in our experiment, which we place in the magnetic field, we are only interested in the anomalous Zeeman effect, as this is what occurs with sodium.

1.5 Selection rules

Now we turn our attention to the selection rules for the electron transitions, as these are the crucial point for understanding the splitting. In Figure 2, a schematic is sketched to exemplify the individual transitions of the hydrogen atom.

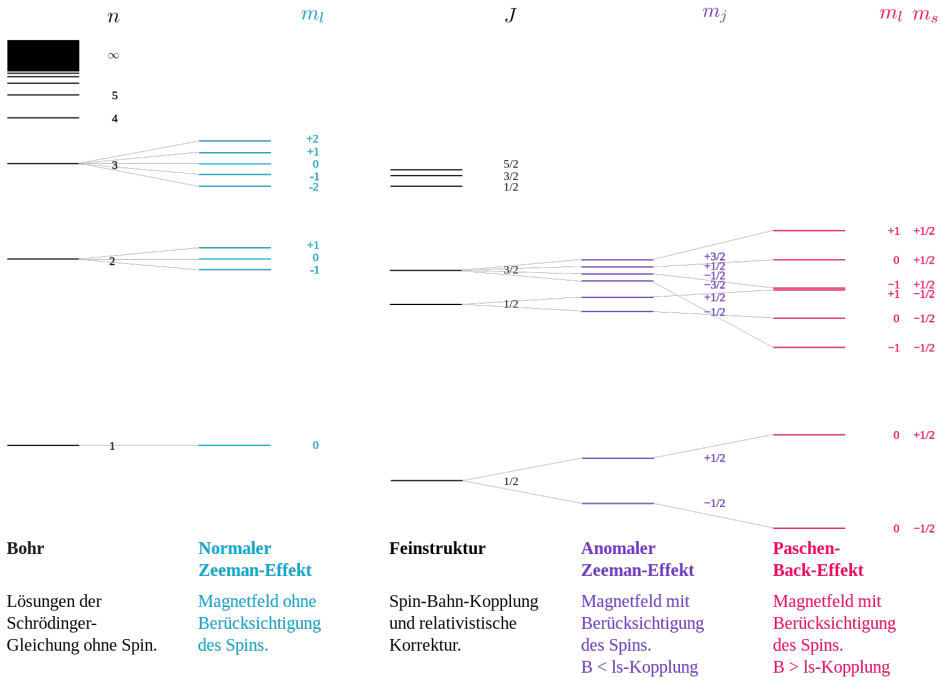

Figure 2: Energieniveaumodell der Aufspaltung beim Wasserstoff

The selection rules always refer to the quantum numbers. This means that we can first establish a non-strict rule that $\Delta n \neq 0$. This is very often the case, but not a particularly important or decisive rule.
The first important rule states that our orbital angular momentum quantum number must change: $\Delta l = \pm 1$. This means that some transitions are not possible if the difference in the l quantum number is greater than 1.
Another selection rule states that the change in the total angular momentum J can only be 0 or 1. The total angular momentum is the combination of spin and orbital angular momentum. The selection rule here is: $\Delta J = 0, \pm 1$, However, it is not allowed to transition from $J = 0 \leftrightarrow J = 0$ even though the difference is also 0.
The next selection rule refers to the magnetic quantum number m, and it states that $\Delta m_J = 0, \pm 1$ With these selection rules in mind, we can predict all possible transitions or determine which transitions are possible. These rules constrain us, and not every transition is possible. This is why, in our experiment, we will later see that we get only two spectral lines for the D_1 transition and six lines for the D_2 transition.

1.6 Strength of Dipole Transitions

In the previous chapters, we have broadly covered the Zeeman effect and attempted to describe it. Now, we examine the strength of dipole transitions. We can view the dipole transition as the coupling between different energy levels with different angular momenta

and a photon, which has a certain energy ΔE. To better describe these transitions, we use the so-called Clebsch-Gordan coefficients.
o better describe these transitions, we use the so-called Clebsch-Gordan coefficients. J_1 and J_2 with different j and m (quantum numbers). The corresponding eigenvectors each form an eigenbasis, and we can simply add the angular momenta $J_g es = J_1 + J_2$. Thus, we can also represent the states of the total angular momentum as a tensor product:

$$|j_1, m_1; j_2, m_2\rangle = |j_1, m_1\rangle \otimes |j_2, m_2\rangle \tag{1}$$

These product states form an orthonormal basis of the total system, therefore, the states can also be represented as linear combinations of the original basis:

$$|J, M\rangle = [\sum_{m_1=-j_1}^{j_1}][\sum_{m_2=-j_2}^{j_2}]|j_1; j_2; m_1, m_2\rangle\langle j_1, j_2; m_1, m_2|J, M\rangle \tag{2}$$

The closing part of the sentence might be referring to the calculation of Clebsch-Gordan coefficients. These coefficients are calculated as follows:

$$\begin{aligned}\langle j_1\, m_1\, j_2\, m_2|J\, M\rangle &= (-1)^{-j_1+j_2-M}\sqrt{2J+1}\begin{pmatrix} j_1 & j_2 & J \\ m_1 & m_2 & -M\end{pmatrix} \\ &= (-1)^{2j_2}(-1)^{J-M}\sqrt{2J+1}\begin{pmatrix} j_1 & J & j_2 \\ m_1 & -M & m_2\end{pmatrix}\end{aligned}$$

Figure 3: Berechnung der Clebsch-Gordan-Koeffizienten

2 Experimental Setup

Next, we will take a closer look at the experimental setup. This consists of several components:

- Sodium spectral lamp in magnetic field
- several lenses
- Lyot-Filter
- FPI
- camera

With that, we have our setup, which we had to adjust before conducting the experiment. Now, we will take a closer look at the Lyot filter and the FPI.

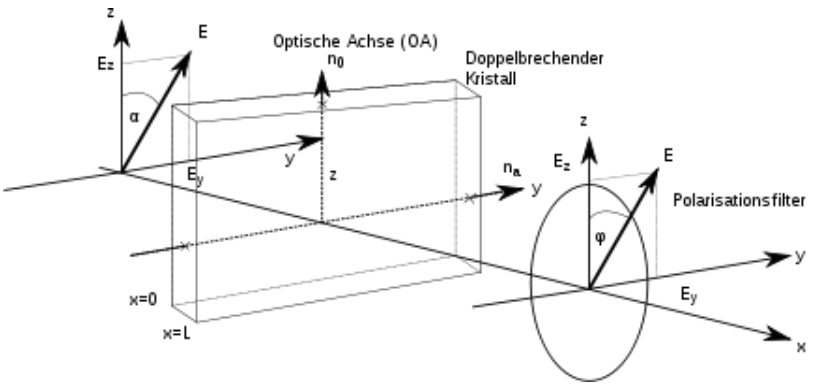

Figure 4: Aufbau und Funktion Lyot-Filter

2.1 Lyot-Filter

The Lyot filter uses birefringent crystals and utilizes the interference of polarized light. The filter consists of this crystal and two polarization filters, which can be rotated relative to each other, thereby making various transitions and parts of the lines (e.g. π- or σ components) visible. The setup is roughly outlined in Figure 4.

This way, we have selected and focused on which parts we examined in the experiment.

2.2 FPI

The FPI (Fabry-Pérot Interferometer) is a high-resolution spectrometer that allows us to visualize our spectral lines.

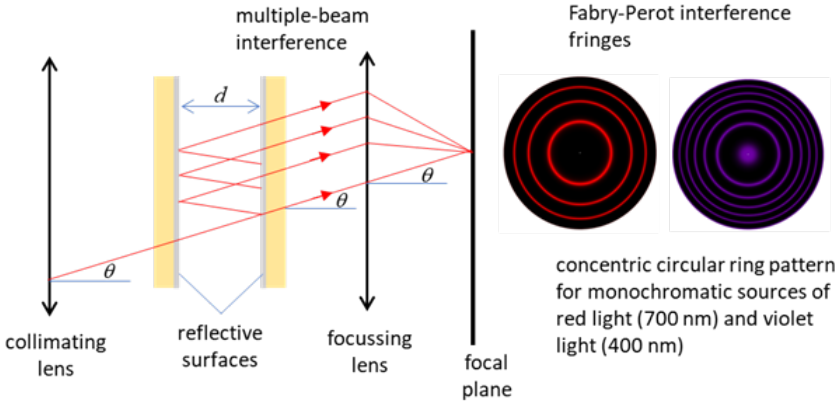

Figure 5: Aufbau und Funktion FPI

As seen in Figure 5, the interferometer consists of two highly reflective glass plates (reflectivity R=0.9), with their reflective sides facing each other on the inside. This allows light to enter and undergo multiple reflections in the space between them. The spacing between the plates can be adjusted using millimeter screws, and the orientation of the mirrors can also be adjusted, which we did during the optical alignment process.
During the multiple reflections, interference occurs, resulting in coherent light. This coherent light is then focused by a lens located behind (with focal length f) onto a plane

(here, a camera). This process generates the characteristic ring patterns, which we can interpret and examine in the following steps.

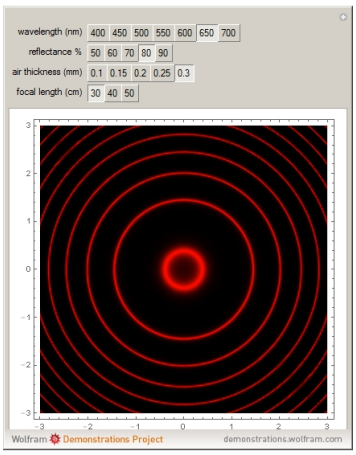

Figure 6: Beispiel eines Interferenzmusters

In this process, depending on how the Lyot filter is adjusted and the strength of the magnetic field, we can observe different divisions of the lines within the rings. This means we can see different transitions.
The remainder of the setup consists of standard components that are already familiar.

3 Analysis

3.1 Calibration of the electromagnet using a Hall sensor

Initially, we measured the homogeneity of the magnetic field at current values of $I_1 = 5A$ and $I_2 = 10A$ and found that the field is relatively homogeneous. The value changed only in the second decimal place.

I_1	I_2
0,49-0,46	0,95-0,91

Table 1: Homogenität des Magnetfeldes

During this process, the Hall sensor was adjusted forwards, backwards, and vertically, and only minor deviations were measured. However, these results are sufficient for our measurements.
Next, we should determine the magnetic induction B as a function of I. We plotted our measured values, and a relatively good straight line can be seen. This means that we can conclude $B \propto I$ indicating that with increasing current strength, we obtain stronger magnetic induction. We have one measurement point that differs significantly from the others. This could either be an error in reading the magnetic field strength or a transmission error in the lab notebook. After fitting our best-fit line, we obtained a slope value of $A = 8,4279 \times 10^{-2} \frac{T}{A}$, which indicates how much our magnetic field increases per ampere. For our final measurements we use a steady current of $I = 10A$ and therefore $B = 0,95T$.

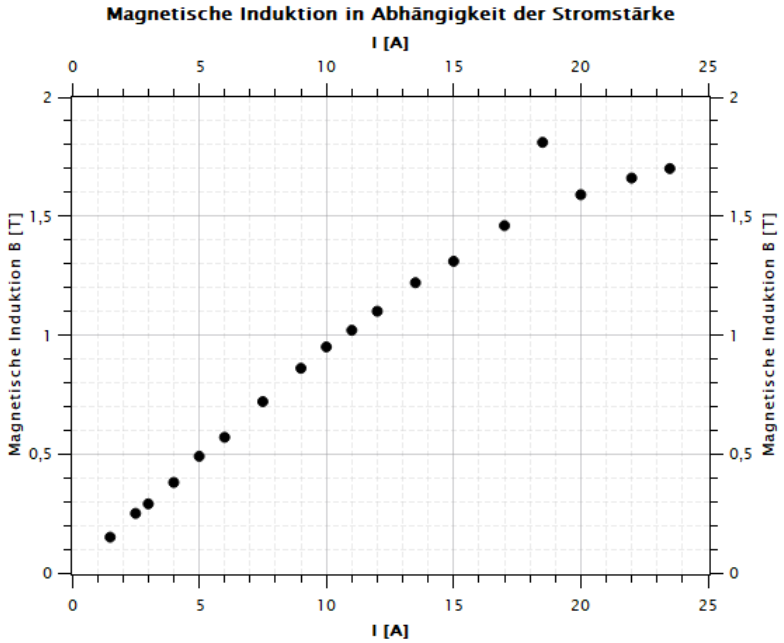

Figure 7: Magnetische Induktion gegen Strom

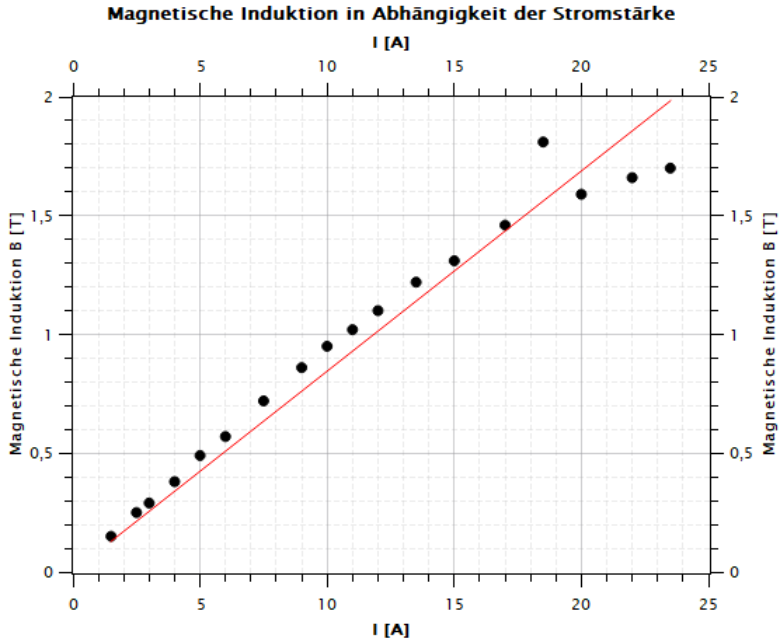

Figure 8: Gerade zur Bestimmung der Steigung

To determine the correction function we need the Peaks at the integervalues without a magnetic field.

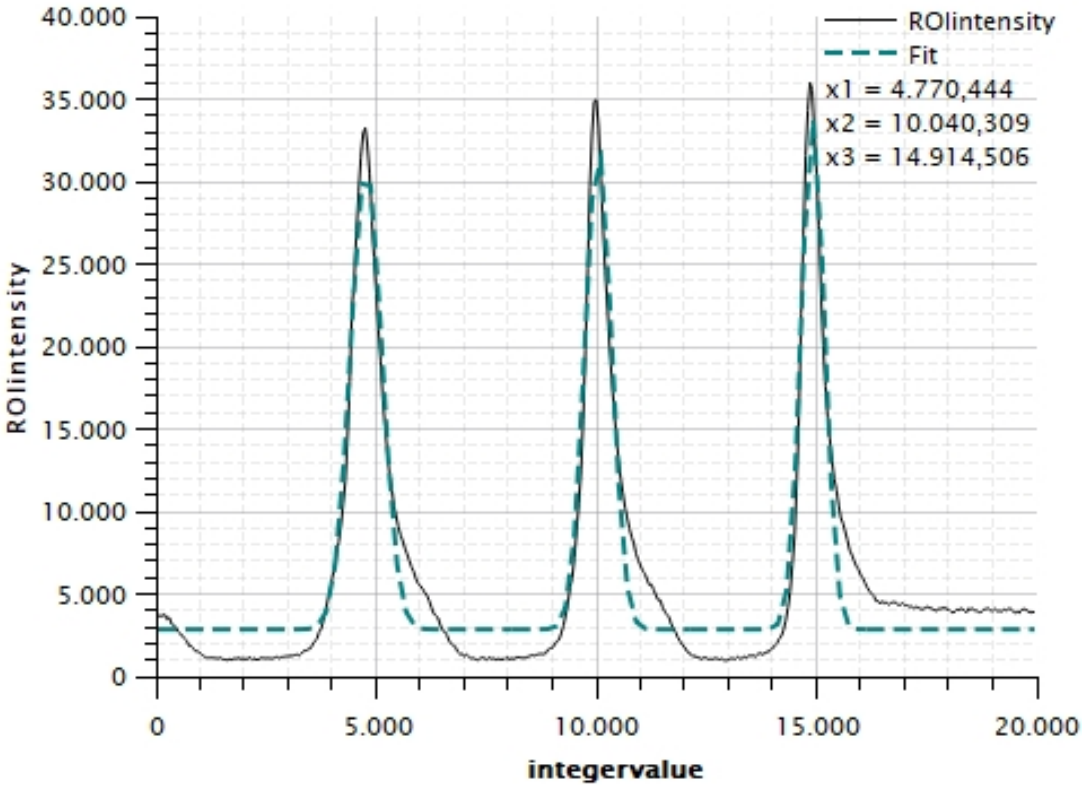

Figure 9: Measurement without magnetic field.

$$\Delta\nu_{FSR} = \frac{c}{2L} = 7,575367912 \cdot 10^{10} \frac{1}{s} \tag{3}$$

With the distance between the plates L and using the difference between the peaks we can now calculate the correction function for determining the frequencies from the integervalues from

$$m = \left(\frac{f_2 - f_1}{I_2 - I_1}\right) = \frac{\nu_{FSR}}{I_2 - I_1}$$

$$f_c(I) = m \cdot I = 1,4955 \cdot 10^{10} \cdot I \tag{4}$$

with I being the integervalue. By using eq (4) we can determine the corresponding frequencies from the integervalue.

3.2 Determination of Landé Factors

The Zeeman energy is given by

$$\Delta E_{\text{Zee}} = m_J g_J \mu_B B \tag{5}$$

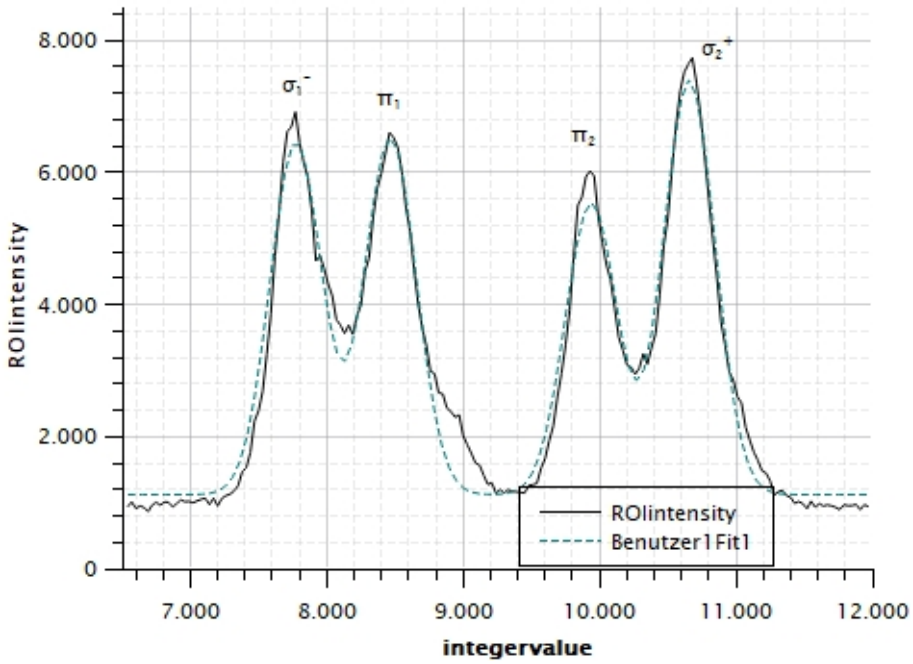

Figure 10: D_1-line from FPI scan with σ- and π-transitions

With $\mu_B \approx 9.274 \times 10^{-24} J/T$ being the Bohr magneton.

By using the ratio of the σ- and π-lines we can now determine the relative displacements. With $\Delta E = h \cdot \Delta f$ we can calculate the difference in the wave lengths and determine the Landé factors g_j for a steady magnetic field $B = 0.95T$.

For D_1 we get equations

$$\frac{\Delta E_{Zee}(\sigma_2^+) - \Delta E_{Zee}(\sigma_1^-)}{\mu_B B} = g(S_{1/2}) + g(P_{1/2})$$
$$\frac{\Delta E_{Zee}(\pi_2^+) - \Delta E_{Zee}(\pi_1^-)}{\mu_B B} = g(S_{1/2}) - g(P_{1/2})$$

And for D_2 we get

$$\frac{\Delta E_{Zee}(\sigma_2^+) - \Delta E_{Zee}(\sigma_1^-)}{\mu_B B} = g(P_{3/2}) + g(S_{1/2})$$
$$\frac{\Delta E_{Zee}(\sigma_2^-) - \Delta E_{Zee}(\sigma_1^+)}{\mu_B B} = g(S_{1/2}) - 3g(P_{3/2})$$
$$\frac{\Delta E_{Zee}(\pi_2) - \Delta E_{Zee}(\pi_1)}{\mu_B B} = g(S_{1/2}) - g(P_{3/2})$$

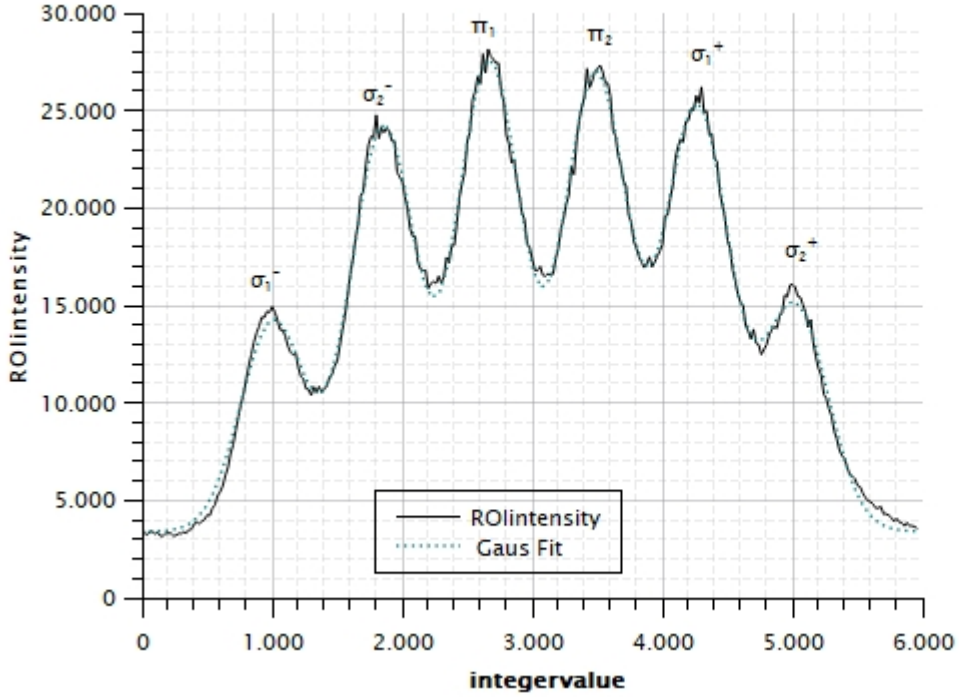

Figure 11: D_2-line from FPI scan with σ- and π-transitions

In the appendix we also plotted the Intensities with the frequencies.

Transition	D_1	D_2	theoretical value
$S_{1/2}$	8036,786884	901,124	2
$P_{1/2}$	8434,473	-	2/3
$P_{3/2}$	-	3597,827031	4/3

Table 2: Caption

Here something went wrong and we got way too big values for the Lande-factors.

3.3 Determination of Clebsch-Gordan Coefficients

At a magnetic field of 0.95T, we recorded the D_2-line and were able to determine the π- and σ-transitions. The curve was formed by a Gaussian fit over the sum of six equally broad Gaussian functions. The squares of the Clebsch-Gordan coefficients represent the probability of transitioning to a system with an excited state. The Clebsch-Gordan coefficients can be determined from the ratios of the intensities of the σ- and π-transitions. The σ_2^- and σ_1^+ transitions have a probability of 1. The remaining coefficients are determined from the intensities of the transitions from the initial state to the excited state.

Transition	Measured Intensity
σ_1^-	0.337359
σ_1^+	1
π_1	0.662641
π_2	0.643612
σ_2^-	1
σ_2^+	0.356387

Table 3: Measured intensities and Clebsch-Gordan coefficients for the D_2-line transitions.

The theoretical values are obtained from the tables for the Clebsch-Gordan coefficients.

Transition	Theoretical Value	Coefficient
σ_1^-	0.5774	0.5808261
σ_1^+	1	1
π_1	0.8165	0.814028
π_2	0.8165	0.802254
σ_2^-	1	1
σ_2^+	0.5774	0.596982

Table 4: Theoretical Clebsch-Gordan coefficients for the D_2-line transitions.

4 References

[1] Prof. Dr. J. Eschner, *Zeeman-Effekt, FoPra*.

[2] Nolting, *Grundkurs Theoretische Physik 5/2*.

[3] Haken & Wolf, *Atom und Quantenphysik*.

[4] NUMERICAL ANALYSIS OF OPTICAL AND ELECTROMAGNETIC PHENOMENA, *FABRY – PEROT INTERFEROMETER*.

[5] Stoppi - Homemade Physics, *Zeeman-Effekt*.

5 Appendix

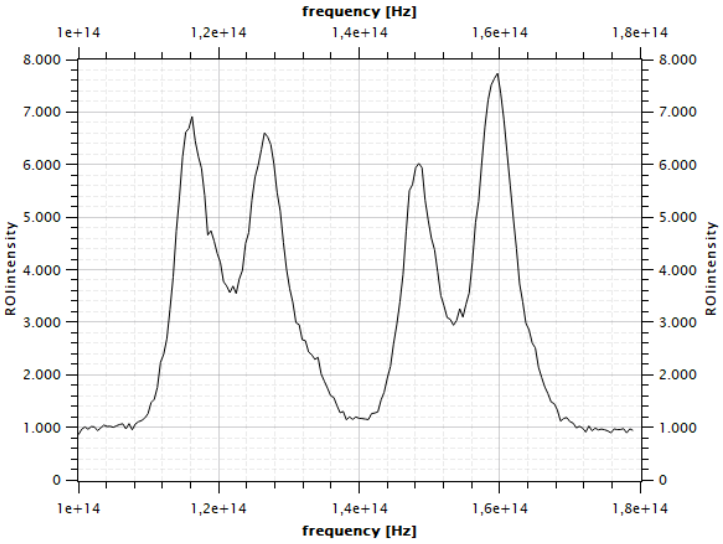

Figure 12: D_1-line with frequencies.

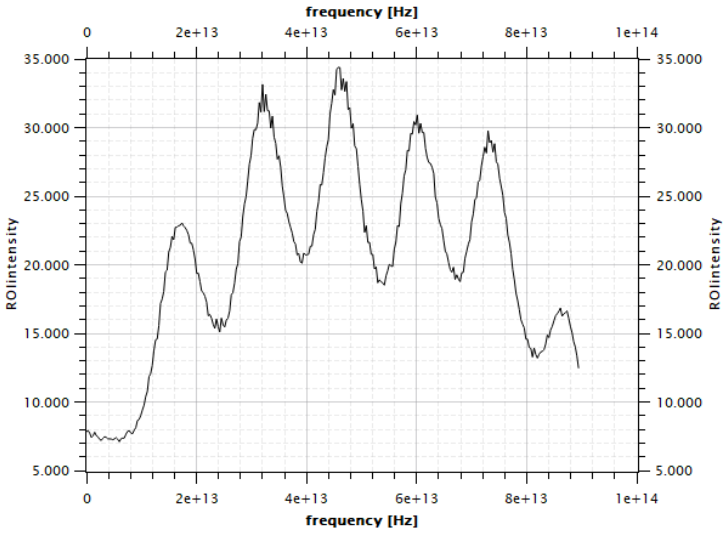

Figure 13: D_2-line with frequencies.